21th International Conference on Renewable Energies and Power Quality (ICREPQ'23)
Madrid (Spain), 24th to 26th May 2023
Renewable Energy and Power Quality Journal (RE&PQJ)
ISSN 2172-038 X, Volume No.21, July 2023

Cosine Windows in Interpolated DFT-based Method for an Accurate High-Frequency Distortion Assessment in Power Systems

A. Bracale[1], P. Caramia[1], G. Carpinelli[2], P. De Falco[1] ad P. Verde[3]

[1] Department of Engineering
University of Naples Parthenope
Centro Direzionale Is. C4, 80143 Naples (Italy)
e-mail: antonio.bracale@uniparthenope.it, pierluigi.caramia@uniparthenope.it, pasquale.defalco@uniparthenope.it

[2] Retired. Former Professor of Electrical Power Systems
Naples, Italy
gcarpin53@gmail.com

[3] Dep. of Electrical and Information Engineering Engineering & DIAEE
University of Cassino and Lazio Meridionale & La Sapienza Università di Roma
Via di Biasio n. 43 - 03043 Cassino (Italy)
e-mail: verde@unicas.it

Abstract.

The transformation of electrical networks in the context of the new smart grid paradigm unavoidably involves new challenges regarding Power Quality (PQ) disturbances not only for customers but also for all the other involved stakeholders. Among PQ disturbances, waveform distortions have recently gained growing interest due to the massive presence of new technologies in distributed energy resources, in modern loads and in advanced smart metering systems. The presence of these devices determines arduous electromagnetic compatibility problems since the current and voltage waveform distortions in smart grids are characterized by spectral components above the traditional 2 kHz frequency limit, in a range extended up to 150 kHz. In this paper, an interpolated DFT-based (IDFT) method, recently proposed in the relevant literature in the field of signal processing, is properly extended for an accurate and fast assessment of power system waveform distortions in the frequency range from 2 to 150 kHz. Since DFT-based methods can suffer well-known spectral leakage problems, in this paper the IDFT is applied using cosine windows that minimize interference conditions among spectral components and maximise the estimation accuracy of the spectral component amplitude, phase angle and frequency. An optimal number of cosine window terms is also searched to improve the spectral analysis of high-frequency power system waveforms. Numerical applications on synthetic test signals and measured waveforms are carried out to quantify the accuracy and computational efforts of the proposed approach and to select the cosine window terms that better optimize the waveform distortion assessment.

Keywords. Power Quality, High-Frequency Waveform Distortion Assessment, Supraharmonics, DFT.

1. Introduction

Modern power systems are undergoing rapid changes with the unavoidable wide deployment of new electrical and communication technologies [1]. Such evolution leads to new challenges in the planning and operation of electrical distribution systems. In this context, particular attention is required in monitoring and assessment of Power Quality (PQ) disturbances due to the wide diffusion of sensitive loads and perturbing equipment [2-5].

Among PQ disturbances, waveform distortions are of great concern and their accurate evaluation is nowadays of particular interest. Indeed, waveform distortions in smart grids can be significantly compromised by the increasing penetration of power converters largely utilized in distributed energy resources (such as wind, solar power plants and storage systems), in electric vehicle chargers, and in modern loads (e.g., adjustable speed drives, LED and fluorescent lamps) [3,6]. These devices can lead to voltage and current waveforms including distortions characterized by a spectral content in a wide range of frequencies, up to 150 kHz. In contrast with the "low-frequency distortion" that usually ranges up to 2 kHz, the spectral content between 2 and 150 kHz is indicated as "high-frequency distortion" or "supraharmonics" [3,6,7].

The high-frequency distortions can cause different problems in the electrical power systems, such as potential interferences with the power-line communication, errors in control systems, possible resonance phenomena and reduction of life of electronic devices and network components. While electromagnetic compatibility coordination in the low-frequency range is well recognized in relevant literature and Standards, the high-frequency range has not been explored as carefully and a standardized measurement technique is nowadays lacking, as the relevant Standards only suggest informative measurement methods for the assessment of grid compliance [8-10].

Several methods have been proposed in the recent relevant literature for waveform distortion evaluation in presence of high-frequency spectral components [11-17]. Both

DFT-based and parametric techniques have been explored: the former methods can suffer well-known spectral leakage problems while the latter methods can be computationally intensive although guaranteeing high result accuracy [16]. Improved performance can be obtained through either Interpolated DFT-based (IDFT) methods and Hybrid Approaches (HAs). IDFT methods estimate the frequency location interpolating two or more DFT output points, reducing the spectral leakage with acceptable computational efforts. HAs try to find the best compromise between accuracy and computational effort [16-17]. An HA example is the profitable strategy of divide and conquer applied in [17] that combines a Discrete Wavelet Transform with a Nuttal sliding-window Discrete Fourier Transform (DFT) and with a modified ESPRIT method.

Nevertheless, in spite of the great evolution of parametric and hybrid methods, we contend that there are still large areas for research in the context of IDFT-based methods, particularly when the object of interest is their application to the assessment of high-frequency distortion in power system waveforms, as it is the case of this paper.

A variety of IDFT-based methods have been proposed in the relevant literature for the signal processing of generic waveforms [18-19]. In [18], the IDFT method weights the analysed signal by suitable cosine windows before applying the IDFT algorithm, aiming at reducing the amplitude attenuation of spectral components and the mutual interference among tones. In our opinion, the use of sliding cosine windows, i.e. windows characterized by a large and flat central lobe, is particularly profitable to assess the high-frequency distortion of power systems waveforms, where the spectral components are usually far apart in the frequency domain.

Motivated by the above, in this paper, an IDFT-based method using a cosine window is applied for an accurate and fast assessment of high-frequency distortion of power system waveforms characterized by a wide frequency range from 2 to 150 kHz. The IDFT-based method is optimized by searching the number of terms of the sliding cosine window that minimizes the interference conditions among high-frequency spectral components, thus maximising the benefits in terms of estimation accuracy of their amplitude, phase and frequency.

The remainder of the paper is organized as follows. The IDFT-based method with a cosine window is described in Section 2 together with an explanation of the procedure to find the optimal number of terms of the cosine sliding window. Section 3 presents numerical applications of the proposed method on synthetic and measured waveforms. The conclusions are in Section 4.

2. The proposed method

The DFT-based methods are most frequently applied to assess waveform distortions, and they are often adopted by Standards and Recommendations. Unfortunately, desynchronization usually occurs in practice and therefore the accuracy returned by these methods is affected by the spectral leakage and picket-fence effect. IDFT-based methods utilizing suitable cosine windows have been proposed to reduce the above problems [18-19]. In IDFT-based methods, the frequency of each spectral component is estimated by interpolating the two largest DFT samples belonging to the corresponding spectrum peak; the related amplitude and phase parameters are then estimated by using the obtained frequency value. The use of a sliding cosine window guarantees excellent frequency resolution, peak sidelobe ratio, and sidelobe decay.

In this paper, we apply the IDFT-based method with a cosine window for an accurate assessment of distortions of power system waveforms characterized by a wide range of high-frequency spectral components. Simple formulas are utilized for estimating the amplitude, phase and frequency of the spectral components considering the presence of cosine windows [19]. An optimal number of cosine window terms is also searched to improve the spectral analysis of high-frequency power system waveforms.

Let us consider a generic waveform $\boldsymbol{x(n)}$ that includes $\boldsymbol{M}$ sinusoidal spectral components and noise. If it is sampled with a constant sampling rate $\boldsymbol{T_s}$, a sequence of $\boldsymbol{N}$ samples can be modelled as follows:

$$x(n) = \sum_{m=1}^{M} A_m \sin(2\pi f_m n T_s + \varphi_m) + \varepsilon(n) \qquad n = 0,1,\dots,N-1 \quad (1)$$

where A_m, f_m and φ_m, are the amplitude, frequency, and phase angle of the m^{th} tone included in the signal and $\varepsilon(n)$ is the noise term.

The application of DFT unavoidably determines the multiplication of the original signal by a sliding window $w(n)$ (the rectangular window is the simplest case). This leads to the waveform $x_w(n) = x(n)w(n)$. The DFT of the resulting signal is given by:

$$X_w(\lambda) = \sum_{m=1}^{M} \frac{A_m}{2j} [W(\lambda - \lambda_m)e^{j\varphi_m} - W(\lambda + \lambda_m)e^{-j\varphi_m}] \qquad \lambda \in [0, L] \quad (2)$$

where L is the number of samples of $x_w(n)$, $W(\lambda)$ is the DFT of $w(n)$ and $\lambda_m = \frac{f_m}{f_s} L$ with $f_s = 1/T_s$.

In power system high-frequency distortion assessment, it is desirable to apply the DFT using a sliding window characterized by a $W(\lambda)$ with a negligible level of sidelobes and with a minimum distance between spectral components larger than the main lobe band. These characteristics can be guaranteed by the cosine windows, often used since they are simple to be implemented and ensure a good leakage reduction capability.

The time domain analytical expression of a sliding cosine window $w(n)$ is:

$$w(n) = \sum_{k=0}^{C-1} (-1)^k a_k \cos\left(2\pi k \frac{n}{L}\right) \quad n = 0,1,\dots,L-1 \qquad (3)$$

where C is the number of terms of the cosine window. In the case of desirable maximum sidelobe decay windows, the coefficients a_k are [20]:

$$a_k = \frac{D_{2C-2}^{C-k-1}}{2^{2C-3}} \quad k = 1,2,\dots,C-1 \quad \text{and} \quad a_0 = \frac{D_{2C-2}^{C-1}}{2^{2C-2}}, \qquad (4)$$

with $D_q^p = \frac{q!}{(q-p)!p!}$.

Under the above assumption, the IDFT-based method with a cosine window can be applied to estimate the amplitudes of spectral components and simple relationships can be

used to evaluate their frequencies and phase angles [19]. These analytical expressions are:

$$\hat{f}_m = \begin{cases} l_m + \frac{(C-1)\alpha_m - C}{\alpha_m + 1}\left(\frac{f_s}{L}\right) & if \; -0.5 \le \delta_m < 0 \\ l_m + \frac{\alpha_m C - C + 1}{\alpha_m + 1}\left(\frac{f_s}{L}\right) & if \;\; 0 \le \delta_m < 0.5 \end{cases} \quad (5)$$

$$\hat{A}_m = \frac{2^{2C-1}\,\pi\delta_m |X_w(l_m)|}{L \sin(\pi\delta_m)(2C-2)!} \prod_{c=1}^{C-1}(c^2 - \delta_m^2) \quad (6)$$

$$\hat{\varphi}_m = angle[X_w(l_m)] - \pi\delta_m + \pi\frac{\delta_m}{L} + -\frac{\pi}{2} sign(\delta_m) - angle[W_0(-\delta_m)] \quad (7)$$

where:

- l_m is the index of the largest amplitude bin corresponding to the m^{th} spectral component;
- $\hat{\delta}_m = \begin{cases} \frac{(C-1)\alpha_m - C}{\alpha_m + 1} & if \; -0.5 \le \delta_m < 0 \\ \frac{\alpha_m C - C + 1}{\alpha_m + 1} & if \;\; 0 \le \delta_m < 0.5 \end{cases}$

  with $\alpha_m = \begin{cases} \frac{|X_w(l_m)|}{|X_w(l_m - 1)|} & if \; -0.5 \le \delta_m < 0 \\ \frac{|X_w(l_m + 1)|}{|X_w(l_m)|} & if \;\; 0 \le \delta_m < 0.5 \end{cases}$
- W_0 is a parameter calculated as shown in [20].

A delicate step in using a cosine window lies in the choice of the parameter C, i.e., the number of terms of the cosine window. In particular, as known [19], increasing C determines that spectrum $W(\lambda)$ is characterized by the rise of main lobe bandwidth and by the decay of sidelobes. This implies that the interference among close tones increases as C increases, while the interference among far tones reduces as C increases. Consequently, in the case of spectral leakage (e.g., desynchronization analysis) the use of increasing C values can reduce the accuracy when a signal is characterized by spectral components close to each other but can improve the accuracy when a signal is characterized by spectral components far from each other.

Note that these considerations are influenced also by other factors, such as spectrum frequency resolution and the number of spectral components in the signals. In fact, a longer duration of sliding windows determines a greater frequency resolution and, thus, a greater distance among spectral components; signals with several spectral components are more susceptible to interference.

In this paper, a study on the parameter C is carried out to obtain the best trade-off between the highest sidelobe decay rate among the cosine windows with the same number of terms and the highest reduction of interference among central lobes.

3. Numerical Applications

This Section aims at applying the proposed method for the analysis of synthetic and measured waveforms characterized by high-frequency distortions. An in-depth analysis is performed to search for the best cosine window, in terms of accuracy and computational effort. Four case studies are reported in the following subsections: the first three cases are related to synthetic waveforms while the last case refers to a measured waveform of a compact fluorescent lamp.

The proposed method, named in the following IDFT-C_k (with k=2, 3, …, 7 being the number of terms of cosine window), is compared in terms of computational time and accuracy with the DFT-based method suggested in IEC 61000-4-7 (IECM) for the analysis of waveforms with high-frequency spectral components [8]. With reference to IECM results, supraharmonics phase angle errors are not reported since they are undefined in the grouping process. All analyses are performed using Matlab® programs developed and tested on a Windows PC with an Intel i7-3770 3.4 GHz and 16 GB of RAM.

A. Case study 1

The synthetic waveform includes a fundamental component with 100 pu amplitude and 50.02 Hz frequency (to introduce desynchronization), and two high frequency spectral components with 1 pu amplitudes and 45° phase angles. The frequency of the first (second) supraharmonic spans the range from 2 kHz to 150 kHz (from 150 kHz to 2 kHz) with a step of 7 Hz, determining 21143 test waveforms. The analysis of these waveforms allows evaluating of the performance of the proposed IDFT-C method with a different allocation of the distortion content and the impact of the interference among supraharmonics on the accuracy. The signals are 1 s long, include white noise with a standard deviation of 0.001 pu and the sampling frequency is 1 MHz.

Table I shows the average percentage errors of the frequencies, amplitudes, and phase angles of the three spectral components obtained with the IDFT-C_k methods and with IECM.

The proposed IDFT-C methods provide the most accurate estimation for all the spectral components. The average errors on supraharmonics are very similar for all cosine windows and it seems that there is no value of parameter *k* guaranteeing better accuracy for this range of frequency. Standard deviations of errors for supraharmonics are also calculated but are not reported here, for brevity: they are smaller than 0.25% for amplitudes, 4.9×10^{-5}% for frequency and 3.6% for phase angles. Also, standard deviations are similar for different values of parameter *k*.

Table I. - Case study 1: frequency, amplitude, and phase angle errors. Bold values indicate the smallest errors.

	Average percentage errors								
	Amplitude			Frequency			Phase angle		
	1	2	3	1	2	3	1	2	3
IDFT-C2	4.4E-05	**2.5E-03**	**2.0E-03**	4.5E-06	**2.9E-07**	**1.6E-07**	**1.0E-04**	4.0E-02	1.7E-02
IDFT-C3	1.6E-05	2.8E-03	2.5E-03	8.7E-07	3.9E-07	1.8E-07	1.4E-04	**3.8E-02**	**1.5E-02**
IDFT-C4	1.6E-05	3.1E-03	2.8E-03	**6.7E-07**	5.0E-07	2.2E-07	1.9E-04	**3.8E-02**	**1.5E-02**
IDFT-C5	1.5E-05	3.4E-03	3.1E-03	7.0E-07	6.1E-07	2.9E-07	2.2E-04	4.4E-02	2.4E-02
IDFT-C6	1.4E-05	3.7E-03	4.1E-03	8.5E-07	7.4E-07	4.4E-07	2.5E-04	5.1E-02	3.4E-02
IDFT-C7	**1.3E-05**	4.1E-03	3.8E-03	1.1E-06	9.6E-07	4.9E-07	2.8E-04	5.7E-02	4.2E-02
IECM	9.4E-03	1.2E+00	1.2E+00	4.0E-02	5.7E-01	5.7E-01	1.5E+02	-	-

The two supraharmonics are characterized by average errors and standard deviation of errors greater than the fundamental component. The analysis of the errors on the 21143 test waveforms highlights that, when the supraharmonics are closer in the frequency domain, a non-negligible interference arises among them. In particular, when supraharmonics are closer than 8 Hz, the amplitudes, frequencies, and phase angle errors increase with the number of cosine windows; this is clearly due to the rise of the main lobe width of the cosine window. These errors are from 17% to 20% for amplitudes, from 0.0012% to 0.007% for frequencies and from 4% to 150% for phase angles. Indeed, 8 Hz is very close to the frequency resolution (5 Hz) and, usually, in power systems applications supraharmonics are farther than 8 Hz.

The analysis of Tab. I shows also that IECM errors are the greatest for all spectral components in the supraharmonics range since they are affected by spectral leakage problems due to the desynchronization of windows of analysis that changes as the supraharmonic frequencies change. On the other hand, the DFT leakage impact on the accuracy of the amplitude estimation is only partially solved by IEC grouping. Supraharmonics allocations, in fact, vary versus time along the 21143 test waveforms so that the IECM errors vary accordingly and they can even reach 70% for both supraharmonics amplitudes, with a large standard deviation (~6%) for both components. On the other hand, grouping deteriorates frequency accuracy leading to frequency errors of 9% for both supraharmonics.

With reference to the computational efforts, IDFT-C methods require about 0.016 s for the analysis of a 0.2 s sliding window. This time does not vary with the parameter *k*, and it is similar to the time required by IECM.

B. Case study 2

Emission with several spectral components with constant frequencies is typical for converters with Pulse Width Modulation (PWM) technology [21]. This case study includes synthetic waveforms constituted by a fundamental component of 10 A at 50.02 Hz and supraharmonics introduced by PWM technique of an inverter with a frequency modulation index m_f (the six components around the $2m_f{}^{\text{th}}$ order); their amplitudes are fixed up to 1.2% of the fundamental (0.03 A, 0.09 A and 0.12 A) in order to emulate the behavior of the PV system during high-irradiance conditions [16]. Phase angles are 45°. To explore the performance of IDFT-C with a different allocation of distortion, m_f changes from 21 to 1491. The signals are 1 s long, include white noise with a 0.001 A standard deviation, and the sampling frequency is 1 MHz. Table II shows the average percentage errors of the amplitudes (Table II.a) and phase angles (Table II.b) of all the spectral components obtained with the IDFT-C_k methods and with the IECM. Figure 1 shows boxplots of amplitude (Fig. 1a) and phase angle (Fig. 1b) error statistics of the supraharmonic with the greatest amplitudes obtained by IDFT-C versus the number of terms of the cosine window. Figure 2 reports the same quantities for the supraharmonic with the smallest amplitudes. Frequency errors are omitted since they are always smaller than $1.5\text{x}10^{-3}$ % for IDFT-C.

With reference to the IDFT-C results in Table II and Figs. 1 and 2, the IDFT-C methods once again provide the most accurate estimation for all the spectral components. Note that the smallest errors occur on supraharmonics with the greatest amplitudes. In Table II, mean amplitude and phase angle errors for all IDFT-C are very similar; however, they slightly reduce from k=2 to k=3 and slightly increase with k > 3. This is coherent with the trade-off interferences occurring as k rises, in the case of several spectral components described in Section 2. Figs. 2a and 2b confirm this consideration since k=3 provides the lowest dispersion for all signals' errors. Similar comments stand also for frequency errors, not reported here for brevity.

Concerning IECM, high values of amplitude errors are due to spectral leakage and the grouping effect that, in some cases, causes the inclusion of more supraharmonics in the same 200 Hz bands. Average frequency errors, here not reported for brevity, are 0.04% for the fundamental and 0.32% for supraharmonics.

Moreover, IECM amplitude and frequency errors have significant variations depending on supraharmonic allocation in the frequency domain, as it was expected. Eventually, the computational time of IDFT-C and IEC are similar (~0.016 s for all test waveforms).

Table II. Case study 2: amplitude (a) and phase angle (b) average errors. Bold values indicate the smallest errors.

(a)

	Average amplitude percentage errors						
	1	2	3	4	5	6	7
IDFT-C2	3.14E-05	3.06E-03	1.06E-03	4.28E-04	4.25E-04	1.06E-03	3.07E-03
IDFT-C3	**1.31E-06**	**3.83E-04**	**1.27E-04**	**9.60E-05**	**9.55E-05**	**1.28E-04**	**3.87E-04**
IDFT-C4	1.61E-06	4.14E-04	1.37E-04	1.03E-04	1.03E-04	1.37E-04	4.12E-04
IDFT-C5	1.53E-06	4.36E-04	1.45E-04	1.09E-04	1.09E-04	1.45E-04	4.36E-04
IDFT-C6	1.44E-06	4.55E-04	1.63E-04	1.14E-04	1.14E-04	1.63E-04	4.56E-04
IDFT-C7	1.35E-06	4.75E-04	1.58E-04	1.18E-04	1.18E-04	1.58E-04	4.74E-04
IECM	0.010	111	35.236	31.157	31.732	37.307	125

(b)

	Average phase angle percentage errors						
	1	2	3	4	5	6	7
IDFT-C2	1.70E-04	6.87E-02	2.25E-02	6.11E-03	6.23E-03	2.26E-02	6.92E-02
IDFT-C3	**2.21E-05**	**3.44E-03**	**1.25E-03**	**9.70E-04**	**9.67E-04**	**1.24E-03**	**3.47E-03**
IDFT-C4	2.40E-05	4.10E-03	1.43E-03	1.12E-03	1.12E-03	1.43E-03	4.11E-03
IDFT-C5	2.77E-05	4.77E-03	1.65E-03	1.28E-03	1.28E-03	1.65E-03	4.78E-03
IDFT-C6	3.07E-05	5.40E-03	1.86E-03	1.43E-03	1.43E-03	1.86E-03	5.42E-03
IDFT-C7	3.34E-05	6.02E-03	2.06E-03	1.58E-03	1.58E-03	2.06E-03	6.03E-03
IECM	158	-	-	-	-	-	-

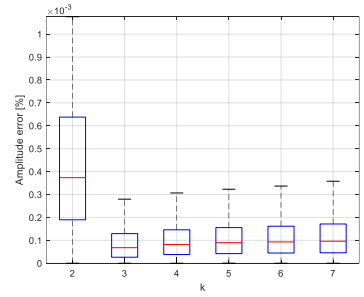

(a)

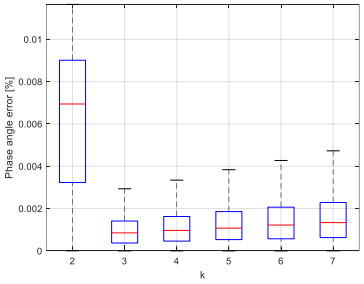

(b)

Fig.1 Case study 2: amplitude (a) and phase angle (b) errors statistics of greatest supraharmonic vs k.

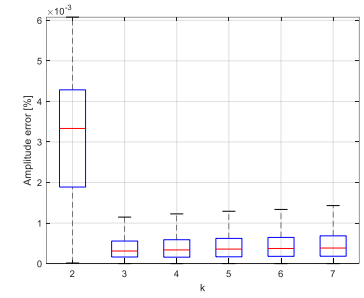

(a)

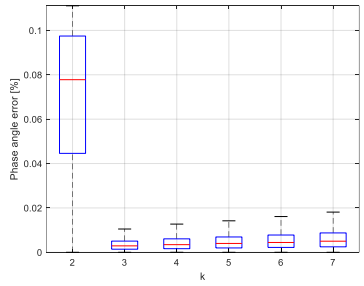

(b)

Fig.2 Case study 2: amplitude (a) and phase angle (b) errors statistics of smallest supraharmonic vs k.

C. *Case study 3*

In this case study an acid test including harmonics, interharmonics and supraharmonics is considered. They are typically low order harmonics due to the background distortion and the dispersed generation systems equipped with inverters utilizing high switching frequencies. The synthetic waveform includes a fundamental of 10 A at 50.02 Hz with all odd harmonics up to the 27th order (low-frequency harmonics), whose amplitudes are in the range [1.4 - 6] % of the fundamental component. The high-frequency content is the one as in Case study 2 with modulation index m_f equal to 201. Eventually, two desynchronized interharmonic tones at frequencies of 17598 Hz and 21997.5 Hz with amplitudes 0.5% of fundamental and white noise with a standard deviation of 0.001 % are added. The signal is 3 s long and its sampling frequency is 1 MHz (Fig. 3 shows the first 200 ms). For brevity, only the amplitudes percentage errors of some spectral components are reported in Table III.

IDFT-C methods outperform IECM. Table III shows that k=2 and k=3 have the best overall performance, although the fundamental and the 13th harmonic have the smallest errors for k=7. Fundamental and 13th harmonic are characterized by the greatest desynchronization conditions due to the highest amplitude (fundamental) and highest harmonic order (13th), and thus the window with the highest sidelobe decay provides the best results. Similar comments stand for frequency and phase angle accuracy. Eventually, the computational time of IDFT-C is 0.017 s, very similar to the time required by the IECM.

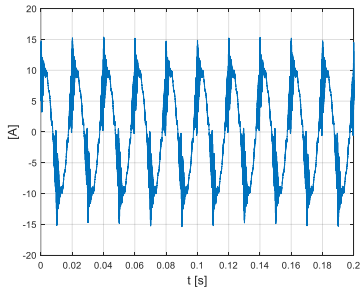

Fig.3 Case study 3: synthetic waveform.

D. *Measured waveform*

The waveform under analysis is obtained from a public database [22] and it is the current signal of a measured compact fluorescent lamp that includes high frequency spectral components up to 50 kHz. The waveform is 0.22 s long, it is sampled at 0.1 MHz and it is reported in Fig 4. In this case study the true values are unknown, thus, to obtain reference values we apply the sliding window Esprit Method (EM) [23], i.e., a pure parametric method characterized by high accuracy but significant computational efforts. The percentage errors of some spectral components are reported in Table IV.

IDFT-C methods again outperform IECM. IDFT-C errors are very similar for all numbers *k* of cosine terms; however smaller k values confirm to be adequate for amplitude and frequency accuracy. Once again, similar comments can be done for frequencies and phase angles IDFT-C accuracy.

Table III. Case study 3: amplitude errors. Bold values indicate the smallest errors.

		Average amplitude errors							
Freq [Hz]	50.02	3rd	5th	7th	9th	11th	13th	17598	21997.5
IDFT-C2	2.07E-05	3.48E-03	4.94E-05	9.43E-04	1.53E-03	1.79E-04	1.56E-04	2.16E-03	**3.78E-03**
IDFT-C3	1.26E-05	**1.05E-03**	**1.51E-04**	**1.60E-03**	1.12E-04	**4.95E-05**	1.93E-04	**2.13E-04**	3.95E-03
IDFT-C4	1.26E-05	1.18E-03	2.16E-04	1.72E-03	**2.78E-05**	8.24E-05	1.28E-04	2.58E-04	4.07E-03
IDFT-C5	1.18E-05	1.25E-03	2.58E-04	1.81E-03	1.46E-04	1.09E-04	9.31E-05	2.82E-04	3.95E-03
IDFT-C6	1.07E-05	1.31E-03	2.77E-04	1.90E-03	2.55E-04	1.33E-04	6.98E-05	2.99E-04	4.02E-03
IDFT-C7	**9.65E-06**	1.37E-03	2.78E-04	1.97E-03	3.53E-04	1.56E-04	**5.30E-05**	3.12E-04	4.26E-03
IECM	0.02	0.32	0.82	1.03	1.46	0.09	0.22	20.03	30.34

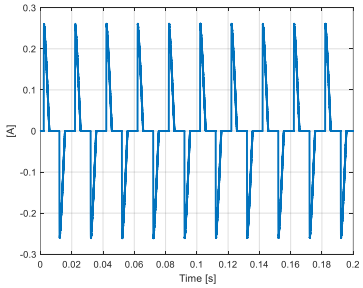

Fig.4 Case study 4: measured waveform.

Table IV. Case study 4: amplitude (a) and frequency (b) errors. Bold values indicate the smallest errors.

(a)

	Amplitude average errors			
Freq [Hz]	3rd	5rd	42.6x10^3	42.7x10^3
IDFT-C2	0.0573	0.0852	0.0250	0.1065
IDFT-C3	0.0574	0.0840	**0.0240**	0.1040
IDFT-C4	0.0570	0.0827	0.0241	0.1003
IDFT-C5	0.0566	0.0813	0.0246	0.0967
IDFT-C6	0.0562	0.0800	0.0251	**0.0935**
IDFT-C7	**0.0558**	**0.0789**	0.0257	0.0907
IECM	0.1623	0.1004	0.0514	0.2619

(b)

	Frequency average errors			
Freq [Hz]	3rd	5rd	42.6x10^3	42.7x10^3
IDFT-C2	**3.70E-05**	0.0142	0.0021	0.0022
IDFT-C3	6.02E-05	0.0142	0.0021	0.0022
IDFT-C4	8.16E-05	0.0142	0.0020	0.0022
IDFT-C5	1.10E-04	**0.0141**	0.0020	0.0021
IDFT-C6	1.44E-04	**0.0141**	0.0020	0.0021
IDFT-C7	1.83E-04	**0.0141**	**0.0019**	**0.0020**
IECM	1.41E-02	0.0538	0.0160	0.0119

Eventually, the computational time of IDFT-C is about 0.015 s, and it is similar to the time required by the IECM.

4. Conclusions

An IDFT-based method proposed in the literature for signal processing is extended for an accurate and fast assessment of power system waveform distortions in the frequency range from 2 to 150 kHz. The IDFT is applied with a different number of terms of the cosine windows to obtain the best trade-off between the highest sidelobe decay rate and the highest reduction of interference among central lobes to maximize the accuracy of the spectral components amplitude, phase angle and frequency. Numerical applications are carried out on test signals and measured waveforms. The main outcomes of the paper are that: (i) the accuracy of IDFT-C is significantly better than the one of IECM for all the number of terms of cosine window; (ii) the computational time of IDFT-C is similar to the IEC method, for all the number of terms of cosine window; (iii) usually, IDFT-C provides similar errors for amplitudes, frequency and phase angles irrespective of the number of terms of cosine window; (iv) in some cases, supraharmonics errors decrease as the number of terms of cosine window decreases.

Eventually, a low value of the number of terms of cosine windows (such as three) is suggested for an accurate and fast estimation of supraharmonics.

References

[1] M. Shabanzadeh, M. P. Moghaddam, “What is the Smart Grid? Definitions, Perspectives, and Ultimate Goals,” *28th Power System Conference*, Tehran, Iran, 4-6 November 2013

[2] C. CIGRE/CIRED JWG, “Power quality and EMC issues with future electricity networks,” in Proc. CIGRE, Mar. 2018, pp. 1–5.

[3] M. H. J. Bollen et al., “Power quality concerns in implementing smart distribution-grid applications,” IEEE Trans. Smart Grid, vol. 8, no. 1, pp. 391–399, Jan. 2017.

[4] De Santis, M.; Di Stasio, L.; Noce, C.; Verde, P.; Varilone, P. Initial Results of an Extensive, Long-Term Study of the Forecasting of Voltage Sags. *Energies* 2021, *14*, 1264

[5] Mottola, F.; Proto, D.; Varilone, P.; Verde, P. Planning of Distributed Energy Storage Systems in μGrids Accounting for Voltage Dips. *Energies* 2020, *13*, 401.

[6] Á. Espín-Delgado, S. Rönnberg, S. Sudha Letha, M. Bollen, “Diagnosis of supraharmonics-related problems based on the effects on electrical equipment,” EPSR journal, Vol. 195, 2021

[7] S. K. Rönnberg et al., “On waveform distortion in the frequency range of 2 kHz-150 kHz—Review and research challenges,” Electr. Power Syst. Res., Vol. 150, pp. 1–10, Sep. 2017.

[8] International Electrotechnical Commission (IEC), “IEC Standard 61000-4-7: General Guide on Harmonics and Interharmonics Measurements, for Power Supply Systems and Equipment Connected Thereto,” IEC, Geneva, Switzerland, 2010

[9] International Electrotechnical Commission (IEC), “IEC Standard 61000-4-30: Testing and Measurement Techniques Power Quality Measurement Methods,” IEC, Geneva, Switzerland, 2015

[10] Specification for Radio Disturbance and Immunity Measuring Apparatus and Methods—Part 1-1: Radio Disturbance and Immunity Measuring Apparatus—Measuring Apparatus, document CISPR 16-1-1:2019, 2019.

[11] T. M. Mendes, C. A. Duque, L. R. M. Silva, D. D. Ferreira, and J. Meyer, “Supraharmonic analysis by filter bank and compressive sensing,” Electric Power Syst. Res., vol. 169, pp. 105–114, 2019.

[12] S. Zhuang, W. Zhao, R. Wang, Q. Wang, and S. Huang, “New measurement algorithm for supraharmonics based on multiple measurement vectors model and orthogonal matching pursuit,” IEEE Trans. Instrum. Meas., vol. 68, no. 6, pp. 1671–1679, 2019.

[13] S. Zhuang, W. Zhao, Q. Wang, Z. Wang, L. Chen, and S. Huang, “A high-resolution algorithm for supraharmonic analysis based on multiple measurement vectors and Bayesian compressive sensing,” Energies, vol. 12, no. 13, p. 2559, Jul. 2019.

[14] S. Lodetti, J. Bruna, J. J. Melero, V. Khokhlov, and J. Meyer, “A robust wavelet-based hybrid method for the simultaneous measurement of harmonic and supraharmonic distortion,” IEEE Trans. Instrum. Meas., vol. 69, no. 9, pp. 6704–6712, Sep. 2020.

[15] A. J. Collin, S. Z. Djokic, J. Drapela, R. Langella, and A. Testa, “Proposal of a desynchronized processing technique for assessing high frequency distortion in power systems,” IEEE Trans. Instrum. Meas., vol. 68, no. 10, pp. 3883–3891, Oct. 2019.

[16] G. Carpinelli, A. Bracale, P. Varilone, T. Sikorski, P. Kostyla, Z. Leonowicz, “A New Advanced Method for an Accurate Assessment of Harmonic and Supraharmonic Distortion in Power System Waveforms” IEEE Access, vol. 9, pp. 88685–88698, 2021

[17] G. Carpinelli, P. Varilone, T. Sikorski, J. Rezmer, P. Kostyła and A. Bracale, "Accurate and Fast Parallelized Assessment of Waveform Distortions in Presence of Low and High frequency Spectral Components," 20th ICHQP, 2022, pp. 1-6

[18] D. Belega, D. Petri, “Fast procedures for accurate parameter estimation of sine-waves affected by noise and harmonic distortion,” Digital Signal Processing, Vol. 114, 2021, 103035

[19] D. Belega, D. Dallet, “Multifrequency signal analysis by Interpolated DFT method with maximum sidelobe decay windows,” Measurement, Vol. 42, Issue 3, 2009, pp. 420-426

[20] D. Belega, “The maximum sidelobe decay windows,” L’Académie Roumaine, Rev. Roumaine Sci. Tech. Sér. Electrotech. Energ., Vol. 50, n. 3, 2005, pp. 349–356.

[21] V. Khokhlov, J. Meyer, A. Grevener, T. Busatto and S. Rönnberg, "Comparison of Measurement Methods for the Frequency Range 2–150 kHz (Supraharmonics) Based on the Present Standards Framework," in *IEEE Access*, vol. 8, pp. 77618-77630, 2020

[22] PANDA database. Available online: http://harmonic-db.wcms-file2.tudresden.de/cgi-bin/PANDA.cgi

[23] A Bracale, G. Carpinelli, I. Y. H. Gu, M. H.J. Bollen, A new joint sliding-window ESPRIT and DFT scheme for waveform distortion assessment in power systems, Electric Power Systems Research, Volume 88, 2012, pp. 112-120.